Proceedings of the 4th International Conference on Environmental Geoscience and Earth Ecology
DOI: 10.54254/2753-8818/2026.33762

Validation and Comparison of Sea Surface Temperature and Salinity Products in the Arctic Ocean

Zizhen Huang

College of Geographical Science, Harbin Normal University, Harbin, China
hzzoxygen@outlook.com

Abstract. Accurate representation of Arctic sea surface temperature (SST) and sea surface salinity (SSS) is an important foundation for in-depth understanding of polar ocean dynamic processes and climate feedback mechanisms. However, systematic evaluations of existing data products are still scarce. This study constructs a unified daily-resolution evaluation framework, and takes the CMEMS in-situ observation dataset as the benchmark truth to systematically assess the thermohaline reconstruction capability of five ocean reanalysis products (G12V1, TOPAZ4, GREP_CGLO, GREP_GLOR and GREP_ORAS) and two satellite retrieval products (AVHRR and BEC) in the Arctic Ocean from 1993 to 2023. The results show that all products generally exhibit high reliability in reconstructing Arctic SST, but a systematic cold bias is widespread, with the most significant errors occurring in summer and multi-year ice zones. For SSS reconstruction, the errors of reanalysis products are most prominent in the estuarine regions of the Siberian shelf, reflecting the persistent inadequacy of current models in depicting the freshwater forcing of terrestrial runoff. The BEC satellite product demonstrates higher accuracy than all reanalysis products within its valid ice-free observation domain. Analysis of the impact of sea ice concentration reveals two distinct error response mechanisms: SST errors increase approximately linearly with rising sea ice concentration, while SSS errors show an inverted V-shaped nonlinear response, with error peaks concentrated in the marginal ice zone. The above findings provide a quantitative basis with physical interpretive significance for the selection of data products under different sea ice conditions, and point out key directions for the improvement of future Arctic ocean-sea ice models and the optimization of satellite retrieval algorithms.

Keywords: Arctic Ocean, sea surface temperature and salinity, ocean reanalysis products, sea ice concentration

1. Introduction

The Arctic Ocean is one of the most sensitive regions to global climate change, and its marine environment has undergone significant changes under the background of global warming [1]. As key variables characterizing the ocean thermal structure and hydrological features, sea surface temperature and sea surface salinity directly affect the formation and ablation of sea ice, and regulate the stability of ocean stratification, air-sea interaction, and the global thermohaline

© 2026 The Authors. This is an open access article distributed under the terms of the Creative Commons Attribution License 4.0 (https://creativecommons.org/licenses/by/4.0/).

DOI: 10.54254/2753-8818/2026.33762

circulation. Therefore, obtaining long-term and accurate Arctic sea surface thermohaline data has become an important foundation for quantitatively evaluating the transformation of ocean thermal structure and climate feedback mechanisms.

Affected by harsh natural environments and complex geographical conditions, in-situ observation data in the Arctic Ocean are relatively scarce. Satellite infrared remote sensing is limited by cloud cover and sea ice occlusion; year-round sea ice coverage prevents Argo floats from operating normally in high-latitude ice zones; and the operating time and scope of research vessels are also very limited. At the same time, the spatial distribution of in-situ observation platforms is unbalanced, with almost no coverage in high-latitude areas such as the central Arctic [2]. This makes it difficult to conduct a comprehensive analysis of the Arctic ocean state relying solely on in-situ observation data.

In recent years, with the development of multi-source observation technology, global ocean reanalysis products have been continuously updated and iterated. For example, ORAS5 developed by ECMWF, GLORYS12V1 developed by Mercator Ocean, and TOPAZ4, a regional assimilation system specially developed for the special polar environment, have been widely used, providing important data support for marine environmental research in polar regions [3-6]. Polar-orbiting satellites such as NOAA equipped with infrared sensors and SMOS equipped with microwave sensors also provide large-scale and high-frequency remote sensing observation products of Arctic sea surface parameters [7]. Uotila et al. [8] systematically evaluated the performance of 10 ocean reanalysis products in the polar regions, pointing out that the multi-model mean (MMM) is superior to single products in depicting the seasonal characteristics of temperature and salinity, but generally underestimates the heat transport to the Arctic. The latest evaluation of 9 Arctic reanalysis products by Yao et al. [9] also indicated that TOPAZ4 and ORAS5 perform well in characterizing the mid-shallow salinity, but there are still significant differences in salinity simulation among various products in key sea areas such as the Barents Sea. Existing studies still have limitations: most evaluation studies take monthly mean fields as the evaluation object, pay insufficient attention to the spatiotemporal distribution characteristics of products on daily indices, and cannot effectively capture short-term anomalous signals in the process of Arctic environmental evolution. Moreover, few existing studies compare reanalysis products and satellite remote sensing retrieval products under a unified framework, leading to unclear advantages and limitations of the two types of products.

Based on the above background, this study establishes a unified evaluation framework to assess the thermohaline reconstruction capability of current high-resolution ocean reanalysis products and satellite retrieval products on the Arctic sea surface. Based on high-quality in-situ observation data, this study systematically quantifies the accuracy of each product from multiple time scales and spatial patterns, and further explores the impact of sea ice concentration on thermohaline errors. This study expects to provide a reliable data selection basis for in-depth understanding of the thermohaline evolution of the polar ocean by revealing the physical laws behind the errors of existing products, and provide scientific references for the optimization of parameterization schemes of future polar ocean models and the iteration of remote sensing retrieval algorithms.

The structure of this paper is as follows: Section 2 introduces the datasets and evaluation methods used; Section 3 presents the accuracy evaluation results of each product in terms of sea surface temperature and sea surface salinity; Section 4 discusses in depth the regulation mechanism of sea ice concentration on thermohaline error characteristics; Section 5 gives the main conclusions and research prospects.

DOI: 10.54254/2753-8818/2026.33762

2. Data and methods

2.1. Reanalysis and remote sensing products

2.1.1. Reanalysis products

The reanalysis products selected in this study are mainly from the Copernicus Marine Environment Monitoring Service (CMEMS). The first is the Global Ocean Reanalysis and Simulation, version 12, version 1 (G12V1) of Mercator Ocean, France. G12V1 has a global high-resolution grid of 1/12° and an advanced multivariate data assimilation scheme, which can provide high-precision three-dimensional physical ocean dynamic fields [4]. The second is the Global Reanalysis Ensemble Product (GREP) [10], including three sub-products: the CMCC Global Ocean Reanalysis System (GREP_CGLO) from the Euro-Mediterranean Center on Climate Change (CMCC) [11]; the Global Ocean Reanalysis and Simulation (GREP_GLOR) from Mercator Ocean [4]; and the Ocean Reanalysis System 5 (GREP_ORAS) from the European Centre for Medium-Range Weather Forecasts (ECMWF) [5]. Finally, the Arctic Ocean and sea ice reanalysis system (TOPAZ4) constructed under the CMEMS framework specifically for the Arctic and North Atlantic regions is an ocean-sea ice coupled data assimilation system, which can provide time-varying and physically consistent estimates of the Arctic ocean state [6].

This study uses the daily data of the above five reanalysis products for analysis, and selects the period from January 1993 to December 2023 as the research period. In terms of horizontal resolution and grid configuration, G12V1 (1/12°, 50 standard levels) and GREP members (1/4°, 75 standard levels) rely on global grids, while TOPAZ4 has customized a 12.5 km polar stereographic projection grid and 50 mixed coordinate layers for the polar regions.

The five reanalysis products differ in model configuration and data assimilation schemes. G12V1 and GREP members are both built based on the NEMO ocean model, while TOPAZ4 adopts the Hybrid Coordinate Ocean Model (HYCOM) to better handle the complex water mass evolution in the Arctic. In terms of air-sea boundary forcing, each system generally uses high-precision ECMWF atmospheric reanalysis data as the external forcing field; TOPAZ4 is driven by 6-hourly ERA5 data throughout the period; G12V1 and the GREP ensemble used ERA-Interim before 2019 and then transitioned to ERA5.

2.1.2. Satellite remote sensing data

This study also selects two satellite retrieval products to obtain daily sea surface temperature data and sea surface salinity data respectively. Among them, the sea surface temperature data adopts AVHRR Pathfinder Version 5.3 L3C (hereinafter referred to as AVHRR) released by NOAA NCEI, and the sea surface salinity data adopts Arctic+ SMOS Level 3 SSS v4.0 [12] (hereinafter referred to as BEC) released by the Barcelona Expert Center (BEC). AVHRR is retrieved from thermal infrared observation data obtained by the Advanced Very High Resolution Radiometer on board the NOAA series of satellites, and its core algorithm is the Nonlinear Sea Surface Temperature (NLSST) algorithm, which corrects atmospheric water vapor attenuation through the brightness temperature difference between the 11 μm and 12 μm channels. A 5-month sliding window dynamic empirical coefficient based on buoy observations is used for calibration during data processing [7]. The spatial resolution of this product is approximately 4 km. BEC is derived from observation data of the MIRAS L-band microwave radiometer on board the SMOS satellite. It adopts the Debiased Non-Bayesian Retrieval method [13] to invert sea surface salinity by minimizing the difference between

DOI: 10.54254/2753-8818/2026.33762

observed and simulated Stokes parameters, thereby reducing the impact of prior constraints on the results. This product introduces Nodal Sampling to reduce microwave radiation interference near the sea ice edge, and performs systematic bias correction based on the WOA2023 climatological field. Its spatial resolution is 25 km (polar stereographic projection grid), the temporal resolution is a 9-day running average, and the data coverage ranges from 2011 to 2022.

2.2. Observation data

The in-situ observation data in this study comes from the In Situ Thematic Assembly Centre (In Situ TAC) of CMEMS. This dataset integrates multi-source marine observation data worldwide. The data integrates in-situ data from various marine observation platforms such as ships, drifting buoys, moored buoys, and Argo profiling floats, including many key physical ocean parameters such as temperature and salinity. All observation data have undergone strict real-time quality control (RTQC) and delayed-mode evaluation and verification before being stored and released, and are assigned corresponding quality control flags (QC flags) [14] to reflect the reliability level of the data.

To establish a reliable benchmark truth, this study first conducts strict cleaning and quality control on the observation data. Since this study focuses on sea surface thermohaline data, only observations within the depth range of 0–1 m are retained. Then, combined with the physical and oceanographic characteristics of the Arctic Ocean, valid values with temperatures ranging from -1.8°C to 40°C and salinity ranging from 0 to 40 psu are retained. In addition, quality identifier filtering is performed, and only observation records with good or fairly good QC flags are retained. Aiming at the irregular spatiotemporal distribution of in-situ observation scatter points, the data after quality control is aggregated into a unified 0.1° × 0.1° latitude and longitude grid. In the daily and per-grid aggregation process, for grids with multiple observations, records with an intra-group range greater than 2 are first screened out, and then data exceeding ±3 times the standard deviation of the mean are eliminated to further ensure data reliability. The average value is taken for the filtered data according to the grid-day combination as the benchmark truth at that spatiotemporal node. Figure 1 shows the spatial distribution of preprocessed observation samples.

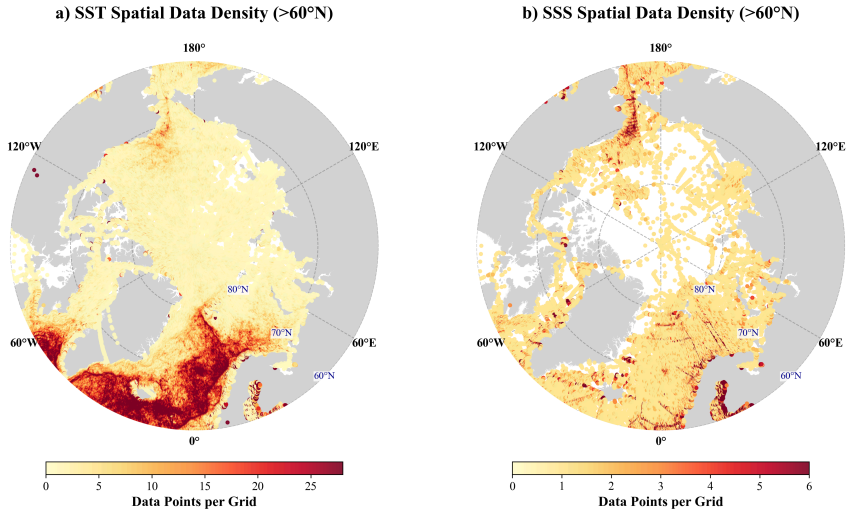


Figure 1. Spatial distribution of SST (a–b) and SSS (c–d) observation samples

DOI: 10.54254/2753-8818/2026.33762

2.3. Sea ice concentration data

Sea ice cover is the main feature of the Arctic Ocean and has a direct interaction with thermohaline processes. Sea Ice Concentration (SIC) refers to the ratio of the area covered by sea ice to the total area of a given sea area. The daily sea ice concentration data used in this paper comes from Version 6 of the Climate Data Record of Passive Microwave Sea Ice Concentration jointly released by the National Oceanic and Atmospheric Administration (NOAA) and the National Snow and Ice Data Center (NSIDC) [15]. This dataset is a long-term, continuous and standardized product processed with climatological consistency. Its core data is mainly the observed brightness temperature data of passive microwave sensors such as the Special Sensor Microwave/Imager (SSM/I) and the Special Sensor Microwave Imager/Sounder (SSMIS), based on the NASA Team (NT) algorithm [16], and combined with the characteristics of the Bootstrap (BT) algorithm [17] for consistency optimization. The data adopts Polar Stereographic projection with a spatial resolution of 25 km × 25 km.

2.4. Data processing methods

To unify the observation data with reanalysis products and remote sensing retrieval products in the spatiotemporal dimension and ensure the accuracy of evaluation results, this study unifies the time of observation samples, reanalysis and remote sensing products to 12:00 UTC on the same day to match data of the same natural day. Meanwhile, the nearest valid value is searched within a radius of 50 km for matching; otherwise, it is invalid. The surface data of each product is uniformly extracted. The sub-members of the GREP ensemble product (GREP_CGLO, GREP_GLOR, GREP_ORAS) are extracted for subsequent comparative analysis.

To quantitatively evaluate the accuracy of each reanalysis product and satellite retrieval product in terms of temperature and salinity in the Arctic Ocean, this study selects three indicators for error analysis of the matched datasets, including Mean Bias (MB), Root Mean Square Error (RMSE) and Centered Root Mean Square Error (CRMSE) [18].

3. Results

3.1. Temperature

3.1.1. Overall accuracy evaluation

Figure 2 is a scatter plot of the accuracy evaluation of sea surface temperature of each product in the Arctic Ocean. The correlation coefficients of all products are above 0.945, indicating a high overall fitting degree. Among them, AVHRR satellite data shows the highest correlation coefficient (0.948) and the smallest RMSE (1.202°C). However, as an infrared satellite sensor, AVHRR cannot penetrate clouds and cannot obtain data in sea ice-covered areas, so its effective matching sample size (N ≈ 715,000) is much lower than that of each ocean reanalysis product (N ≈ 2.16 million). This suggests that the high accuracy of AVHRR may largely benefit from the fact that its evaluation data are concentrated in ice-free open waters with relatively stable hydrological conditions. In contrast, reanalysis products G12V1, TOPAZ4 and the GREP ensemble achieve a high spatial coverage of over 97% while maintaining high correlation. Within the GREP products, GREP_CGLO and GREP_ORAS have low CRMSE, 1.273°C and 1.284°C respectively, while GREP_GLOR has a relatively high CRMSE of 1.327°C. In addition, TOPAZ4 has the highest CRMSE, reaching 1.361°C. It is worth noting that the mean bias of each product is negative, indicating an overall cold

DOI: 10.54254/2753-8818/2026.33762

bias, with AVHRR having the largest bias (-0.415°C) and G12V1 the smallest (-0.202°C). Overall, each product shows high reliability in simulating sea surface temperature, but there is a systematic cold bias.

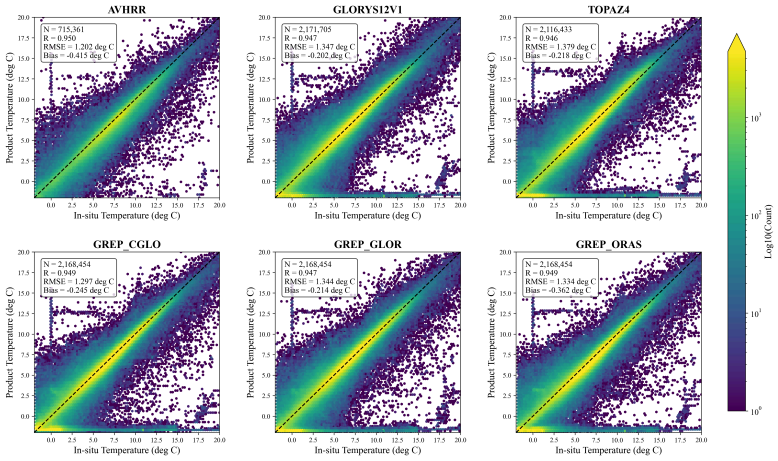


Figure 2. Scatter plot of accuracy evaluation of Arctic sea surface temperature products

3.1.2. Spatial distribution characteristics of errors

Figure 3 shows the spatial distribution of the mean bias of all evaluated products. Each reanalysis product shows an obvious cold bias in the main multi-year ice regions of the Arctic (areas north of the Canadian Arctic Archipelago and Greenland), with a mean bias ranging from -1.6°C to -2.0°C. In addition, except for TOPAZ4, each reanalysis product has a more severe cold bias in the Yenisei Bay and Ob Bay regions of Russia, with an average below -3.0°C. In contrast, the bias of the AVHRR satellite retrieval product has no significant spatial characteristics, mainly because its available quantity in sea ice-covered areas is much less than that of reanalysis products.

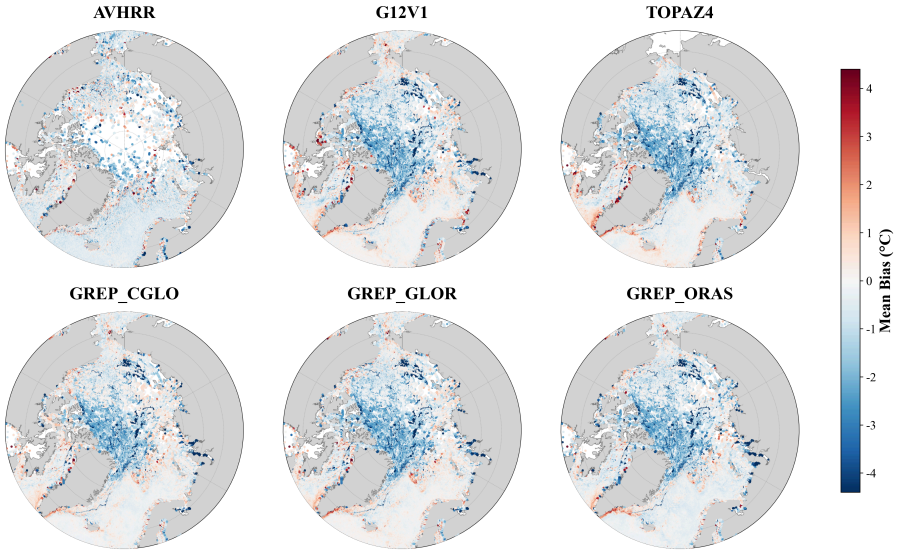


Figure 3. Spatial bias distribution map of Arctic sea surface temperature products

DOI: 10.54254/2753-8818/2026.33762

3.2. Salinity

3.2.1. Overall accuracy evaluation

In terms of sea surface salinity, the performance differences among products are significantly enlarged. All products show obvious positive bias, with the bias ranging from 0.544 to 0.850 psu, indicating that the simulation results are generally too saline (Figure 4). Among the reanalysis products, TOPAZ4 performs the best, with a correlation coefficient of 0.979 (Figure 4), and the lowest RMSE and CRMSE among reanalysis products. In contrast, products such as G12V1 and GREP_CGLO have large errors, with CRMSE exceeding 2.5 psu, and the highest degree of dispersion from the observation data. As a remote sensing product, BEC has fewer effective observations in ice zones, so the effective matching number is about 45% of that of each reanalysis product. In these effective observations, the BEC product shows a high level of accuracy, with MB and RMSE superior to each reanalysis product.

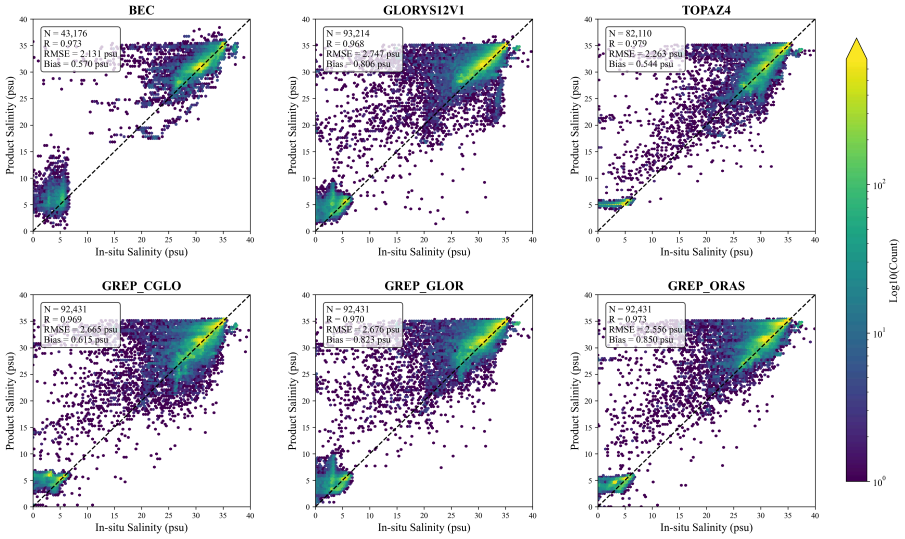


Figure 4. Scatter plot of accuracy evaluation of Arctic sea surface salinity products

3.2.2. Spatial distribution characteristics of errors

Figure 5 shows that the salinity error presents obvious regional heterogeneity in space. Among them, reanalysis products show significant positive bias in the shallow waters of the Russian Arctic shelf and obvious positive bias in the Beaufort Sea and Chukchi Sea. In the shelf areas of the Kara Sea and Laptev Sea, especially in the estuarine areas of large rivers, reanalysis products such as G12V1 and GREP show significant positive bias. The mean bias in this region is as high as 2.0 psu, and the local maximum bias even exceeds 2.3 psu. In the Chukchi Sea and Beaufort Sea regions, most reanalysis models also show obvious positive bias, mainly ranging from 0.5 to 1.6 psu. BEC satellite retrieval salinity shows an inconsistent spatial error distribution. In marginal seas such as the East Siberian Sea, especially near the sea ice edge, when reanalysis products are too saline, BEC data show a certain negative bias.

DOI: 10.54254/2753-8818/2026.33762

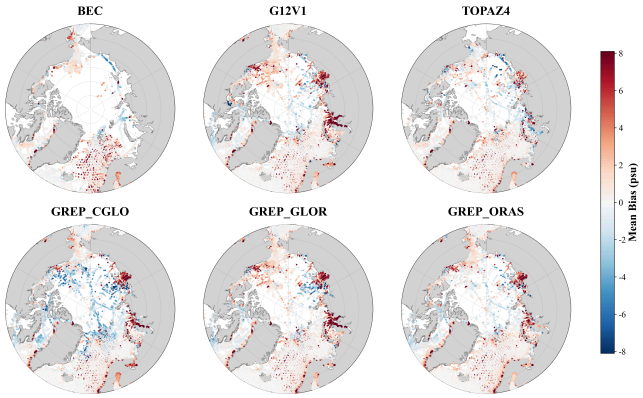


Figure 5. Spatial bias distribution map of Arctic sea surface salinity products

4. Discussion

Arctic thermohaline products show strong spatiotemporal heterogeneity in the evaluation. This study believes that the spatial clustering and temporal fluctuation of these errors are deeply affected by sea ice concentration. As Xie et al. [19] pointed out, the spatial error distribution of TOPAZ4 in the Arctic region is often significantly affected by the sea ice boundary and the number of assimilated observations.

4.1. Characteristics of temperature error variation with sea ice concentration

Figure 6 shows that with the increase of sea ice coverage, the RMSE and bias of sea surface temperature of all products show an approximately linear and significant increasing trend. In ice-free or low-ice open waters (SIC < 15%), each product performs relatively well, with RMSE ranging from 0.900 to 1.157°C and bias ranging from -0.413 to 0.003°C. This benefits from factors such as abundant in-situ observation data in open waters. In dense ice zones (SIC > 80%), the errors increase significantly, with RMSE rising to between 1.933 and 2.961°C, accompanied by a cold bias ranging from -1.832 to -0.951°C. The physical shielding of dense sea ice invalidates satellite infrared and microwave observations, and the assimilation system degrades due to the lack of large-scale surface data constraints. Since current models are imperfect in depicting sub-ice thermodynamic processes such as penetrating shortwave radiation, ice-bottom roughness and latent heat of phase change, a severe systematic cold bias is finally caused in dense ice zones.

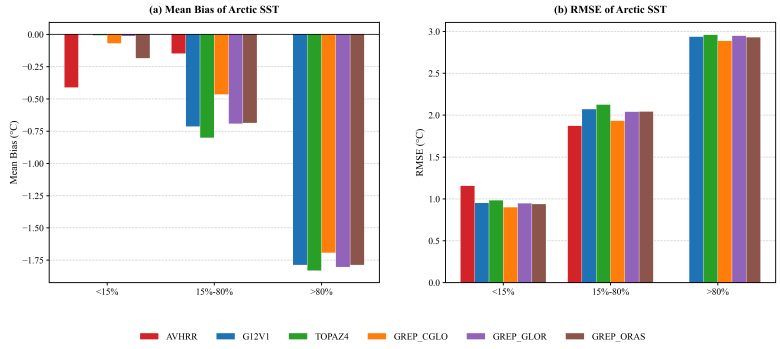


Figure 6. Evolution characteristics of Arctic sea surface temperature product errors with sea ice concentration

DOI: 10.54254/2753-8818/2026.33762

4.2. Characteristics of salinity error variation with sea ice concentration

The response of sea surface salinity to sea ice concentration shows a significant inverted V-shaped nonlinear characteristic. The maximum error of salinity simulation does not occur in dense ice zones, but is highly concentrated in the marginal ice zone with intense ice-water phase change (Figure 7). When the sea ice concentration is in the transition interval of 15%–80%, the salinity RMSE of each product reaches 3.292–5.757 psu, accompanied by a positive bias of 0.149–1.872 psu. The marginal ice zone is the area with the most intense air-sea-ice thermodynamic interaction in the polar regions, where freshwater released by summer ice melting and brine rejection during winter freezing generate extremely strong local freshwater flux forcing. However, current numerical models often produce severe overestimation bias due to the limitations of parameterization schemes when resolving such subgrid-scale intense phase changes and accompanying strong salinity stratification. In addition, for satellite remote sensing products, mixed pixels with 15%–80% sea ice concentration are highly likely to cause a severe "sea ice contamination" effect, leading to the general failure of the retrieval algorithm of L-band microwave radiometers in the marginal ice zone. It is worth noting that when the sea ice concentration exceeds 80%, the overall RMSE of salinity of each product drops to 2.404–4.925 psu, which is significantly lower than the error extreme value in the marginal ice zone. Compared with the high-frequency dynamic mixing and alternate freezing and thawing in the marginal ice zone, the water stratification under dense ice is relatively stable, and the freshwater flux changes gently.

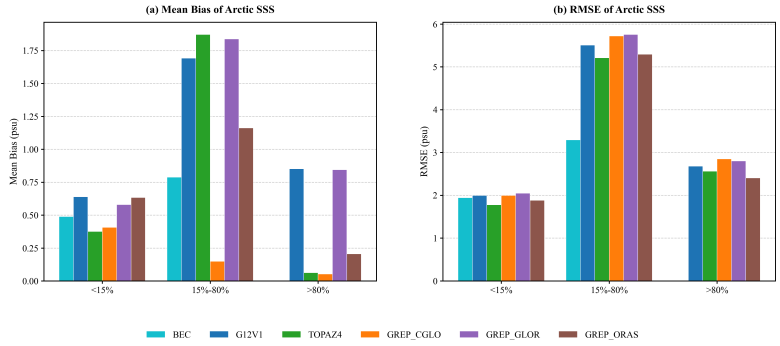


Figure 7. Evolution characteristics of Arctic sea surface salinity product errors with sea ice concentration

5. Conclusions

Through comparison with observation data, this study conducts a detailed evaluation and analysis of the sea surface temperature and salinity data of five reanalysis products (G12V1, TOPAZ4, GREP_CGLO, GREP_GLOR and GREP_ORAS) and two satellite retrieval products (AVHRR and BEC) in the Arctic Ocean. The main conclusions are as follows:

1. In terms of sea surface temperature reconstruction, each product has high overall reliability, but a systematic cold bias is widespread, and the errors are most significant in summer and multi-year ice zones. Affected by sea ice, SST errors increase approximately linearly with the increase of sea ice concentration, which is mainly attributed to the physical shielding of satellite observations by dense sea ice and the insufficient simulation of sub-ice thermodynamic processes by models. Comparing different products, the AVHRR satellite product has the highest observation accuracy in ice-free open waters, but its effective coverage is greatly limited by clouds and sea ice; reanalysis products have more advantages in the integrity of spatial coverage and temporal continuity.

DOI: 10.54254/2753-8818/2026.33762

2. In terms of sea surface salinity reconstruction, each product shows obvious positive bias with significant performance differences. Errors are concentrated in the estuarine areas of the Russian Arctic shelf and the marginal ice zone with intense air-sea-ice interaction. The response of SSS errors to sea ice presents an inverted V-shaped nonlinear characteristic, which reflects the limitations of current models in resolving terrestrial runoff forcing and subgrid-scale freshwater fluxes driven by ice melting and brine rejection. Among reanalysis products, TOPAZ4, specially optimized for polar regions, has the best overall performance; the BEC satellite product has higher accuracy than reanalysis products in its effectively observed ice-free open waters.

In summary, reanalysis products and satellite products have their own advantages in Arctic thermohaline reconstruction: reanalysis products provide near-full spatial coverage and multi-decadal temporal continuity, suitable for full-Arctic long-term climatological analysis; satellite products have higher observation accuracy in open waters, but have gaps in spatial coverage due to constraints of clouds, sea ice occlusion and microwave radiation contamination in the marginal ice zone. For different ocean variables and research needs, data products with stronger pertinence should be preferentially selected to ensure the reliability of research conclusions on the Arctic marine environment.

References

[1] Serreze, M. C., & Barry, R. G. (2011). Processes and impacts of Arctic amplification: A research synthesis. Global and Planetary Change, 77(1–2), 85–96. https: //doi.org/10.1016/j.gloplacha.2011.03.004

[2] Smith, G. C., Allard, R., Babin, M., Bertino, L., Chevallier, M., Corlett, G., Crout, J., Davidson, F., Delille, B., Gille, S. T., Hebert, D., Hyder, P., Intrieri, J., Lagunas, J., Larnicol, G., Kaminski, T., Kater, B., Kauker, F., Marec, C., … the WWRP PPP Steering Group. (2019). Polar Ocean Observations: A Critical Gap in the Observing System and Its Effect on Environmental Predictions From Hours to a Season. Frontiers in Marine Science, 6, 429. https: //doi.org/10.3389/fmars.2019.00429

[3] Balmaseda, M. A., Mogensen, K., & Weaver, A. T. (2013). Evaluation of the ECMWF ocean reanalysis system ORAS4. Quarterly Journal of the Royal Meteorological Society, 139(674), 1132–1161. https: //doi.org/10.1002/qj.2063

[4] Lellouche, J.-M., Greiner, E., Le Galloudec, O., Régnier, C., Benkiran, M., Testut, C.-E., Bourdallé-Badie, R., Drévillon, M., Garric, G., & Drillet, Y. (2018). The Mercator Ocean Global High-Resolution Monitoring and Forecasting System. In E. P. Chassignet, A. Pascual, J. Tintoré, & J. Verron (Eds.), New Frontiers in Operational Oceanography. GODAE OceanView. https: //doi.org/10.17125/gov2018.ch20

[5] Zuo, H., Balmaseda, M. A., Tietsche, S., Mogensen, K., & Mayer, M. (2019). The ECMWF operational ensemble reanalysis–analysis system for ocean and sea ice: A description of the system and assessment. Ocean Science, 15(3), 779–808. https: //doi.org/10.5194/os-15-779-2019

[6] Sakov, P., Counillon, F., Bertino, L., Lisæter, K. A., Oke, P. R., & Korablev, A. (2012). TOPAZ4: An ocean-sea ice data assimilation system for the North Atlantic and Arctic. Ocean Science, 8(4), 633–656. https: //doi.org/10.5194/os-8-633-2012

[7] Casey, K. S., Brandon, T. B., Cornillon, P., & Evans, R. (2010). The Past, Present, and Future of the AVHRR Pathfinder SST Program. In V. Barale, J. F. R. Gower, & L. Alberotanza (Eds.), Oceanography from Space (pp. 273–287). Springer Netherlands. https: //doi.org/10.1007/978-90-481-8681-5_16

[8] Uotila, P., Goosse, H., Haines, K., Chevallier, M., Barthélemy, A., Bricaud, C., Carton, J., Fučkar, N., Garric, G., Iovino, D., Kauker, F., Korhonen, M., Lien, V. S., Marnela, M., Massonnet, F., Mignac, D., Peterson, K. A., Sadikni, R., Shi, L., … Zhang, Z. (2019). An assessment of ten ocean reanalyses in the polar regions. Climate Dynamics, 52(3–4), 1613–1650. https: //doi.org/10.1007/s00382-018-4242-z

[9] Yao, C., Yan, Y., Zhou, Y., Xiong, Z., Xu, Y., & Uotila, P. (2025). Comparative analysis of multiple ocean reanalysis datasets in the Arctic. Climate Dynamics, 63(9), 347. https: //doi.org/10.1007/s00382-025-07842-1

[10] Storto, A., Masina, S., Simoncelli, S., Iovino, D., Cipollone, A., Drevillon, M., Drillet, Y., Von Schuckman, K., Parent, L., Garric, G., Greiner, E., Desportes, C., Zuo, H., Balmaseda, M. A., & Peterson, K. A. (2019). The added value of the multi-system spread information for ocean heat content and steric sea level investigations in the

DOI: 10.54254/2753-8818/2026.33762

CMEMS GREP ensemble reanalysis product. Climate Dynamics, 53(1–2), 287–312. https: //doi.org/10.1007/s00382-018-4585-5

[11] Storto, A., & Masina, S. (2016). C-GLORSv5: An improved multipurpose global ocean eddy-permitting physical reanalysis.

[12] Garcia-Espriu, A., González-Gambau, V., Olmedo, E., Sánchez-Urrea, M., González-Haro, C., Umbert, M., De Andrés, E., Gabarró, C., Turiel, A., Guimbard, S., Bertino, L., Raj, R. P., Catany, R., & Sabia, R. (2026). ESA Arctic+ Salinity Product v4: Enhanced Retrievals Near the Ice-Edge. IEEE Journal of Selected Topics in Applied Earth Observations and Remote Sensing, 19, 5357–5371. https: //doi.org/10.1109/JSTARS.2026.3653416

[13] Martínez González, J., Gabarró, C., & Turiel, A. (2020). Arctic Sea Surface Salinity L2 orbits and L3 maps (V.3.1) [Dataset] [NetCDF]. CSIC - Instituto de Ciencias del Mar (ICM). https: //doi.org/10.20350/DIGITALCSIC/12620

[14] Szekely, T., Gourrion, J., Pouliquen, S., & Reverdin, G. (2019). The CORA 5.2 dataset for global in situ temperature and salinity measurements: Data description and validation. Ocean Science, 15(6), 1601–1614. https: //doi.org/10.5194/os-15-1601-2019

[15] Windnagel, A., Meier, W., & Fetterer, F. (n.d.). NOAA/NSIDC Climate Data Record of Passive Microwave Sea Ice Concentration Version 6 Updates.

[16] Cavalieri, D. J., Gloersen, P., & Campbell, W. J. (1984). Determination of sea ice parameters with the NIMBUS 7 SMMR. Journal of Geophysical Research: Atmospheres, 89(D4), 5355–5369. https: //doi.org/10.1029/JD089iD04p05355

[17] Comiso, J. C. (1986). Characteristics of Arctic winter sea ice from satellite multispectral microwave observations. Journal of Geophysical Research: Oceans, 91(C1), 975–994. https: //doi.org/10.1029/JC091iC01p00975

[18] Taylor, K. E. (2001). Summarizing multiple aspects of model performance in a single diagram. Journal of Geophysical Research: Atmospheres, 106(D7), 7183–7192. https: //doi.org/10.1029/2000JD900719

[19] Xie, J., Bertino, L., Counillon, F., Lisæter, K. A., & Sakov, P. (2017). Quality assessment of the TOPAZ4 reanalysis in the Arctic over the period 1991–2013. Ocean Science, 13(1), 123–144. https: //doi.org/10.5194/os-13-123-2017